CHARACTERIZATION AND POTENTIAL SUITABILITY OF *SIMAROUBA GLAUCA* SEED SHELL LIGNOCELLULOSIC BIOMASS AS ADSORBENT OF BASIC DYES FROM AQUEOUS SOLUTIONS

JEYAGOWRI BALAKRISHNAN[*] and YAMUNA RANGAIYA THIAGARAJAN[**]

[*]*Department of Chemistry, Hindusthan College of Engineering and Technology, Coimbatore, India*
[**]*Department of Chemistry, KIT – Kalaignarkarunanidhi Institute of Technology, Coimbatore, India*
✉ *Corresponding author: J. Balakrishnan, gowrivasu2007@gmail.com*

Received October 5, 2020

The present study investigates the potential of *Simarouba glauca* seed shell powder as a cost-effective adsorbent for the removal of the cationic dyes Malachite green (MG), Methylene blue (MB) and Rhodamine B (RB) from aqueous solutions. The adsorbent was characterized by Fourier transform infrared spectroscopy (FTIR), scanning electron microscopy (SEM) and X-ray diffraction (XRD), as well as by Brunauer–Emmett–Teller (BET) and elemental (CHNS) analyses. Batch mode adsorption studies were carried out varying the experimental conditions, such as initial dye concentration and contact time, adsorbent dose, pH and particle size, in order to assess the adsorbent capacity for the removal of cationic dyes from wastewater. The experimental data were analysed using the Langmuir, Freundlich, Temkin and Dubinin–Radushkevich isotherms. The data fitted well the Langmuir model for the dyes studied. Kinetic data were analysed using the pseudo-first order, pseudo-second order, intraparticle diffusion and Boyd models. The experimental results showed that the pseudo-second order model fitted well.

Keywords: biosorption, *Simarouba glauca* seed shell, cationic dyes, adsorption isotherm, kinetic studies

INTRODUCTION

Water is an essential resource for life. With the help of science and technology, mankind is reaching new horizons in many sectors, but the cost that is paid or will be paid in the near future for these achievements will be too high.[1] Among the consequences of this rapid growth, environmental pollution has become a major and most urgent problem, with critical implications.[2] Water pollution with toxic compounds is one of the major concerns for human health as well as for environmental quality. The main source of water pollution can be attributed to discharge of untreated sanitary and toxic industrial wastes, dumping of industrial effluents and runoff from agricultural fields. Nowadays, with the rapid development of modern industries, the contamination of water associated with dyes present in the effluents of various industries, such as dyeing, printing, textile, leather and coating industries, has drawn much attention.[3] Though industries such as paper and pulp mills, dyestuff, distilleries and tanneries produce highly colored wastewater, it is the textile industry that contributes the most to water pollution with the discharge of large quantities of aqueous waste and dye effluents.

Dyeing wastewaters contain strong color, high amounts of suspended solids, broadly fluctuating pH, high BOD and COD values. Dyes are usually of synthetic origin and have complex aromatic structure, which makes them highly stable and more difficult to biodegrade.[4] The discharge of dye wastewater imparts color to receiving streams and affects their aesthetic value. Dyeing wastewaters interfere with the penetration of sunlight into water, retarding photosynthesis, inhibit the growth of aquatic biota and interfere with the solubility of gases in water bodies.[5]

Dyeing wastewater can be treated by numerous methods, such as adsorption, coagulation, advanced oxidation, membrane separation, aerobic and anaerobic microbial degradation. Among all these methods, adsorption emerged as a cost-effective and eco-friendly technology, with several advantages, such as low initial cost, simplicity in design, ease of operation

and efficient removal of pollutants from wastewater. Activated carbon is commercially used as an adsorbent due to its capability to efficiently adsorb a broad range of adsorbates.[6] Despite its wide use, the application of activated carbon is restricted due to its high cost. Thus, studies pertaining to alternative low-cost adsorbents have emerged in order to replace activated carbon in pollution control through the adsorption process.

Agricultural residues are a viable option as raw materials for the development of adsorbents for water treatment, as they are economic and eco-friendly, as well as due to their unique chemical composition, abundant availability, renewability and reduced disposal costs. Numerous agricultural wastes/by-products, such as raw Brazil nut shell,[7] wood apple shell,[8] walnut shell,[9,10] maize cob,[11,12] sugar beet pulp,[13] coir pith,[14] sawdust[15,16] and sugarcane bagasse,[17] have been investigated as adsorbents for the removal of dyes.

The present study explores the potential feasibility of *Simarouba glauca* seed shell powder for the removal of cationic dyes Malachite green, Methylene blue and Rhodamine B from aqueous solution. *Simarouba glauca* is commonly known as paradise tree or Laxmitaru, it belongs to the Simaroubaceae family native to North America, now found in different regions of India, such as Orissa, Karnataka and Gujarat. *Simarouba glauca* is an edible oil seed bearing tree, well suited for warm, humid and tropical regions. This tree, with its well-developed root system and evergreen dense canopy, efficiently prevents soil erosion and supports soil microbial life. The seed contains about 50-60% oil, with 63% unsaturated fatty acids, among which 59.1% is oleic acid, which is suitable for human consumption. The oil is also used in the manufacture of soaps, lubricants, paints and cosmetics. The oilseed cake, rich in nitrogen, serves as good organic manure. The efficient production of biodiesel from *Simarouba glauca* seed oil has been investigated by several researchers.[18] The present study uses *Simarouba glauca* seed shell for the removal of basic dyes MG, MB and RB from aqueous solutions.

EXPERIMENTAL

Materials

Simarouba glauca seed shells were collected from Gujarat, India. Basic dyes, such as Malachite green (MG), Methylene blue (MB) and Rhodamine B (RB), were chosen for the present study. The dyes Malachite green and Methylene blue were purchased from SFCL Limited, New Delhi, and the dye Rhodamine B was purchased from SD Fine Chem Limited, Mumbai. Stock solutions of the dyes were prepared by dissolving 1.0 g of dye in 1000 mL of double distilled water to obtain the concentration of 1000 mg/L. The stock solutions were diluted to known initial concentrations of the dyes using double distilled water.

Preparation and characterization of raw *Simarouba* seed shell powder (RSS)

Simarouba glauca seed shells were washed with water and dried in sunlight. The dried seed shells were ground to fine powder and stored in an air tight container. The seed shell powder was washed with distilled water several times until the wash water was clear, and then dried in a hot air oven at 60 °C for 24 h. The dried seed shell powder was sieved to different particle sizes (<75 µm, 75-150 µm and >150 µm), and stored in an air tight plastic container for further studies.

Fourier transform infrared spectroscopy (Shimadzu, model IR Affinity-1) analysis of the adsorbent before and after adsorption was performed to determine the surface functional groups and their participation in the adsorption process. The nature and surface characteristics of the adsorbent were analysed by X-ray diffraction (XRD) analysis using an X'Pert PRO X-ray diffractometer (PANalytical B.V., Almelo, the Netherlands). The surface morphology of the adsorbent was investigated by a scanning electron microscope (SEM, JSM-6390, JOEL). The surface area, pore volume and pore size distribution of the adsorbent were determined by the N_2 adsorption–desorption isotherm at 77 K using a BET (Brunauer, Emmett and Teller) surface area analyzer (Micromeritics ASAP 2020). The elemental analysis of the adsorbents was carried out using an Elementar Vario EL III. The pH_{zpc} of the adsorbent was also determined.

Batch mode adsorption studies

Batch adsorption experiments were carried by adding 0.1 g of adsorbent (RSS) into 250 mL Erlenmeyer flasks containing 50 mL of different initial dye concentrations. The flasks were agitated in a rotary shaker at 30 ± 2 °C until equilibrium was attained. The adsorbent was separated by centrifugation and the concentration of the dyes in the supernatant was determined at λ_{max} 617, 667 and 547 nm for MG, MB and RB, respectively, using a visible spectrophotometer (Shimadzu Visible Spectrophotometer UVmini-1240V).

The amount of dye adsorbed onto the adsorbent was calculated by the following equation:

$$q_e = [(C_0 - C_e) \times V]/ M \quad (1)$$

where q_e is the amount of dye adsorbed at equilibrium time (mg/g), C_0 and C_e are the initial and equilibrium

dye concentrations (mg/L), respectively, in solution. V is the volume (L) of solution and M is the mass of adsorbent (g).

RESULTS AND DISCUSSION

Characterization of the adsorbent

The main components of the *Simarouba* seed shell powder are cellulose, hemicelluloses and lignin. The FT-IR spectrum of RSS (Fig. 1) shows a broad band around 3402 cm^{-1} due to the stretching vibration of hydrogen bonded O–H group in cellulose. The peaks observed at 2926 cm^{-1} and 1328 cm^{-1} correspond to the C–H stretching and bending vibration of methyl groups of cellulose and hemicelluloses, respectively. The absorption band at 1722 cm^{-1} is characteristic of the carbonyl group stretching in hemicelluloses.[19] The absorption bands at 1616 cm^{-1} and 1516 cm^{-1} were due to aromatic C=C stretching in the phenyl ring of the lignin structure. The absorption band at 1422 cm^{-1} may be attributed to the methoxy group of lignin in RSS. The strong band at 1034 cm^{-1} also confirms the lignin structure of RSS. The absorption band at 1234 cm^{-1} may be due to the C–O stretching in phenols.[20,21]

Table 1 clearly shows the FT-IR spectral analysis data before and after adsorption. The FT-IR spectra of the dye loaded adsorbents (Fig. 2) show changes in intensity and slight shifting in the position of the peaks. The shift in the position of the peaks corresponding to the C–H bending vibration of methyl groups of hemicelluloses, -C=O stretching in hemicelluloses, aromatic C=C stretching in the phenyl ring of lignin and -(OCH_3) group of lignin confirms the interaction of these functional groups of the adsorbent with the dye molecules.

Scanning electron microscopy was employed to observe the morphological features and surface characteristics of the adsorbents. SEM studies also revealed the surface texture and porosity of the adsorbent materials. Figure 3a shows an uneven, porous and rough surface for RSS, which facilitates the adsorption of dye molecules onto the adsorbent surface. The SEM images of the dye loaded adsorbents (Fig. 3b, 3c and 3d) reveal smooth surfaces, as the pore cavities were covered with the dye molecules.

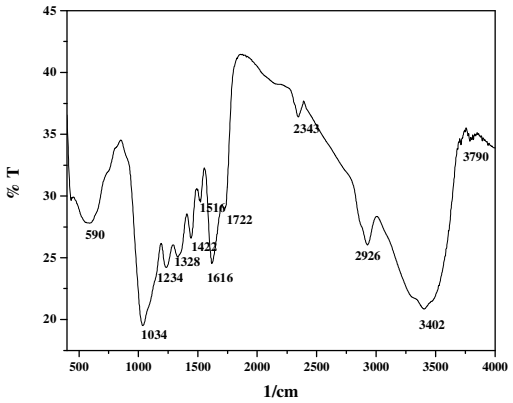

Figure 1: FT-IR spectrum of RSS

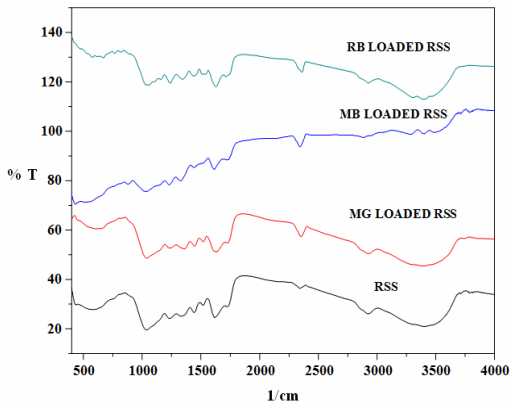

Figure 2: FT-IR spectra of dye loaded RSS

Table 1
FTIR characteristics of RSS

Functional group	Wavenumber (cm^{-1})			
	RSS	MG-RSS	MB-RSS	RB-RSS
-(OH) stretching	3402	3398	3400	3396
-(CH) stretching (cellulose)	2926	2927	2885	2926
-(CH) bending (hemicelluloses)	1328	1359	1327	1346
-(CO) stretching	1722	1726	-	1714
-C=C aromatic (lignin)	1616	1629	1608	1629
-C=C aromatic (lignin)	1516	1517	-	1514
-(OCH_3) (lignin)	1422	1446	1438	1435
-(C-O) stretching	1234	1238	1230	1240

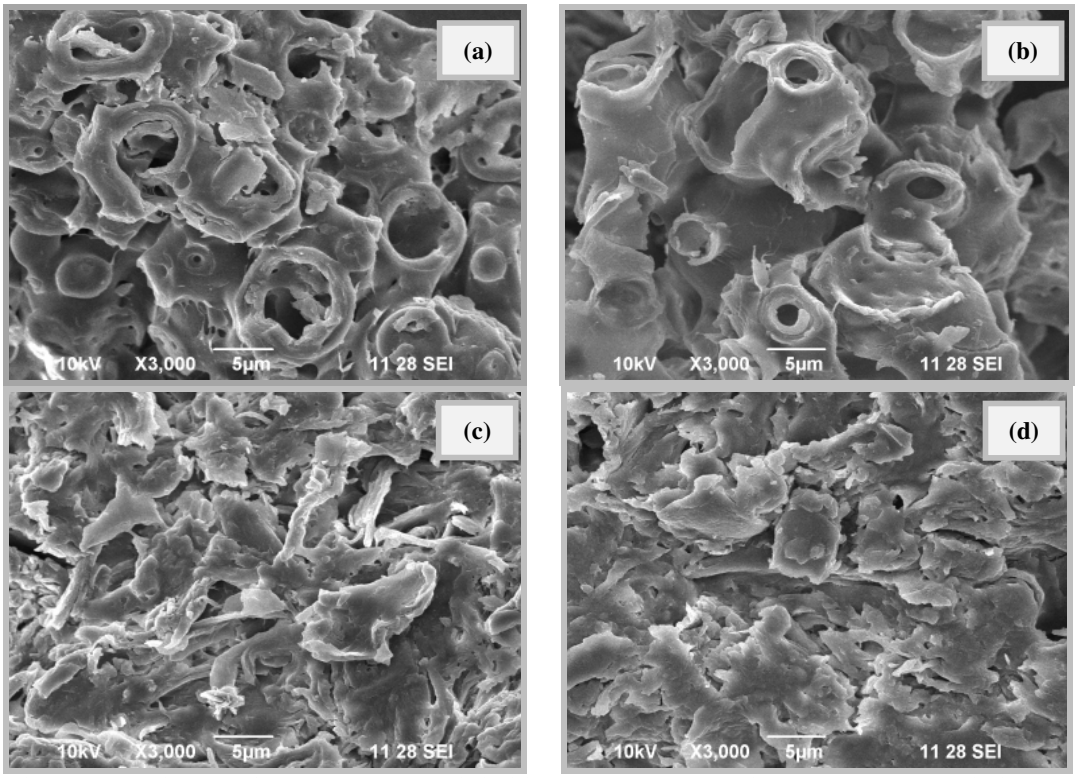

Figure 3: SEM images of a) RSS, b) RSS loaded with RB, c) RSS loaded with MG, d) RSS loaded with MB

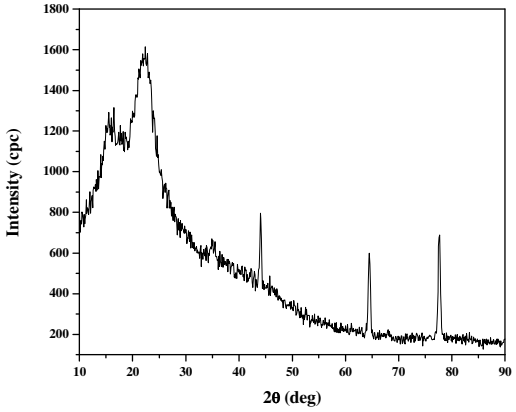

Figure 4: XRD pattern of RSS

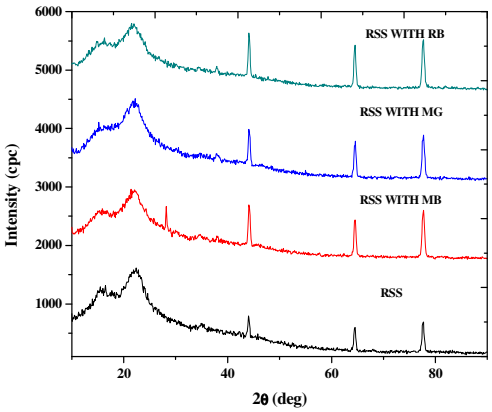

Figure 5: XRD pattern of dye loaded RSS

X-ray diffraction (XRD) is a powerful technique to analyze the crystalline or amorphous nature of materials. Normally, in XRD patterns, well-defined sharp peaks correspond to crystalline constituents, whereas amorphous ones exhibit broad peaks. Figure 4 shows the XRD pattern of the adsorbent RSS. The adsorbent possesses a complex structure, with both crystalline and amorphous regions. The XRD pattern of RSS is similar to those of other cellulosic materials. The largest peak (at around 22^0) indicates the presence of highly organized cellulose, whereas the smallest peak (at around 16^0) indicates the presence of a less organized polysaccharide structure.[22]

When the dye molecules get adsorbed onto the adsorbent, the crystalline nature of the adsorbent undergoes significant changes. Figure 5 shows the diffraction pattern of the dye loaded RSS. The XRD pattern of the dye loaded adsorbent shows

an increase in intensity of the characteristic peaks, which indicates an improvement in the crystalline nature of the adsorbent, probably due to crystal growth as a result of the dye sorption reaction.

Figure 6 shows the pore size distribution of the adsorbent and Table 2 presents the BET surface area and average pore diameter. It is clear that most of the pores of the three prepared adsorbents were in the mesoporous range, which has been confirmed by the average pore diameter. The elemental analysis of RSS was also done and the composition is shown in Table 2.

Effect of initial dye concentration and contact time

The initial dye concentration provides an important driving force to overcome mass transfer resistances of all molecules between the aqueous and solid phases.[23] The contact time between the adsorbate and the adsorbent is of great importance in wastewater treatment by adsorption. The contact time required to reach the equilibrium state depends on the initial dye concentration and the adsorption capacity increases with the initial dye concentration. A rapid uptake of dyes, with a short equilibrium time, decides the efficiency of the adsorbent for its use in wastewater treatment. The effects of initial dye concentration and contact time on the adsorption of MG, MB and RB dyes onto the adsorbent RSS are shown in Figure 7. The contact time curve for the adsorption of MG, MB and RB onto RSS is smooth and continuous, leading to saturation due to the intraparticle diffusion process. The removal of dyes by adsorption onto RSS is initially rapid, then it proceeds at a slower rate and finally attains saturation. At the saturation point, the amount of dye adsorbed reaches a state of dynamic equilibrium with the amount of dyes in the solution.[17] The phenomenon of rapid dye uptake in the initial period of contact time can be explained by the fact that a large number of surface sites are available for adsorption, while after a period of time, the remaining surface sites are difficult to occupy because of the repulsive forces between the solute molecules in solid and bulk phases.[24]

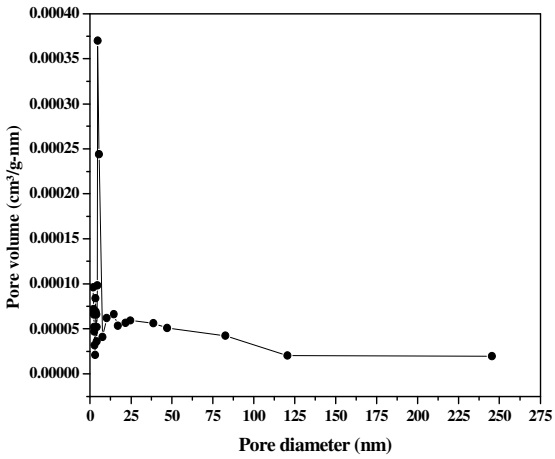

Figure 6: Pore size distribution of RSS

Table 2
Physicochemical characterization of RSS

Parameters	Values
BET surface area	2.0307 m^2/g
Total pore volume	0.004100 cm^3/g
Average pore diameter	12.243 nm
Zero point charge (pH_{zpc})	3.4
C %	51.40
H %	6.036
N %	1.01
S %	0.12

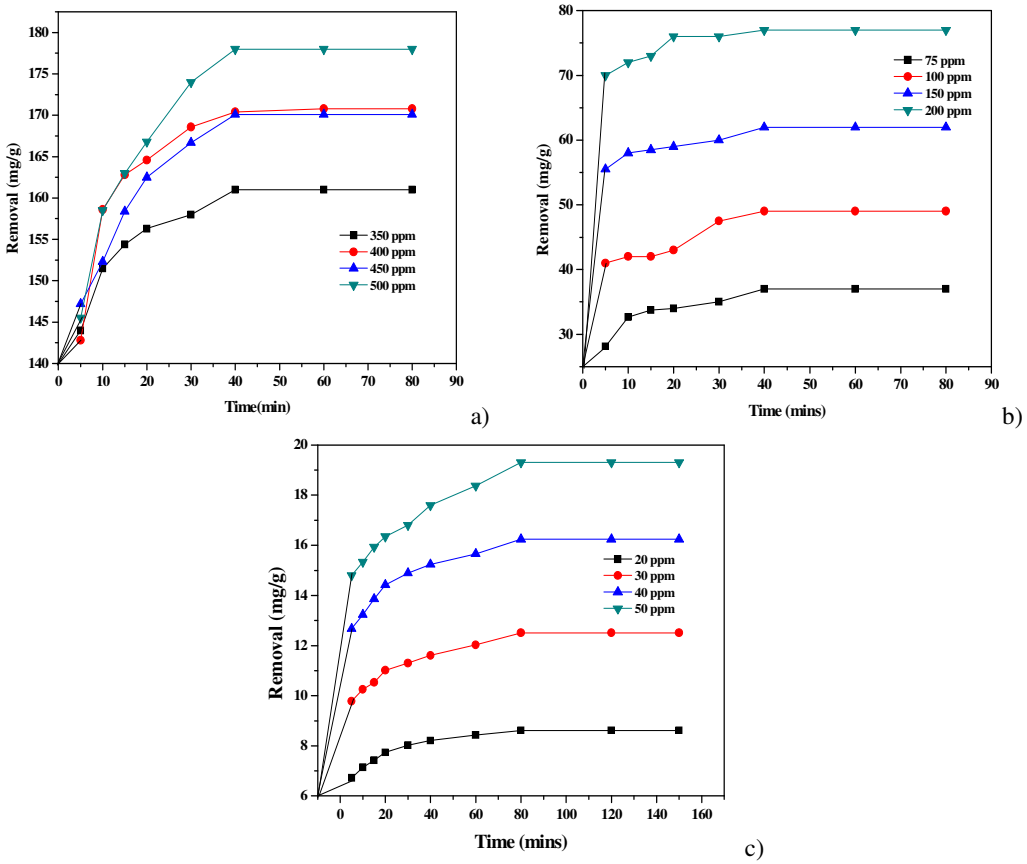

Figure 7: Effect of contact time and initial dye concentration on adsorption of a) MG, b) MB, and c) RB onto RSS (adsorbent dose = 0.1 g/50 mL)

Effect of pH

The influence of **(b)** olution pH on the removal of dye molec ı be explained based on the pH at the point zero charge (pH_{zpc}) of the adsorbent. The pH_{zpc} is a convenient index, showing the pH of the solution when the surface of the adsorbent has zero charge. When the pH of the solution is lower than pH_{zpc}, the surface of the adsorbent becomes positively charged, and when the pH of the solution is greater than pH_{zpc}, the surface becomes negatively charged.[25] The pH_{zpc} of RSS was found to be 3.4. The adsorption of MG, MB and RB by RSS was studied over the pH range of 2-11. From Figure 8, it can be observed that the adsorption capacity of RSS, in the case of MG and MB adsorption, increased, as the pH value rose from 2 to 8, and remained constant with further increase in pH from 10 to 11. This is probably due to the fact that at pH < pH_{zpc}, the surface becomes positively charged, the concentration of H^+ ions is high and they compete with the dye cations for vacant adsorption sites, causing a decrease in dye uptake. At pH > pH_{zpc}, the adsorbent surface becomes negatively charged and favours the uptake of cationic dyes due to an increased electrostatic force of attraction. The influence of pH in the case of RB removal by RSS shows the opposite trend, the increase in pH decreases the adsorption capacity of RSS. The amount of RB adsorbed increased from pH 2 to 4, while further increase in pH from 4 to 11 decreased the adsorption of RB. The higher uptake of RB at lower pH may be probably explained by the fact that excess H^+ ions yielded the zwitterionic molecular form of the dye, enabling the dye molecules to attach to the negative sites of the adsorbent. The decrease in adsorption at pH>4 may be due to the aggregation of the zwitterionic molecular form of RB, generating dimmers, which are unable to enter the pores of the adsorbent.[26] a similar effect has been observed for adsorption using waste coir pith,[27] sago waste carbon,[28] activated carbon from bagasse pith[29] and *Turbinaria conoides*.[30]

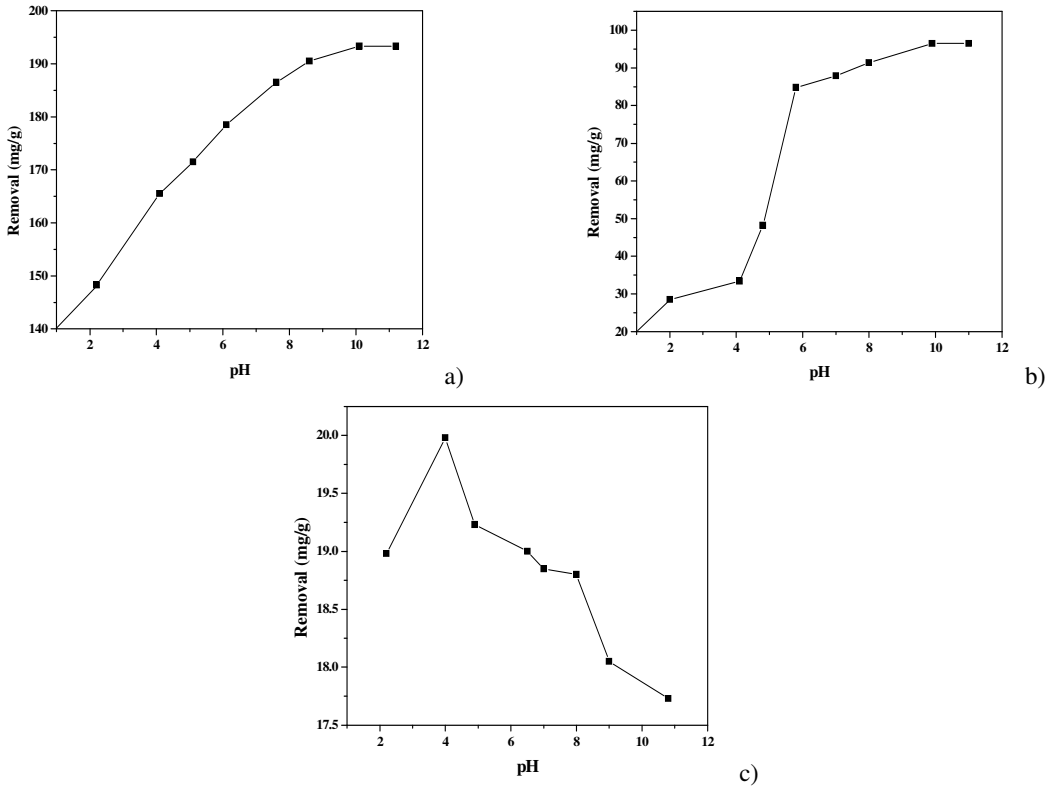

Figure 8: Effect of pH on adsorption of a) MG, b) MB, and c) RB onto RSS

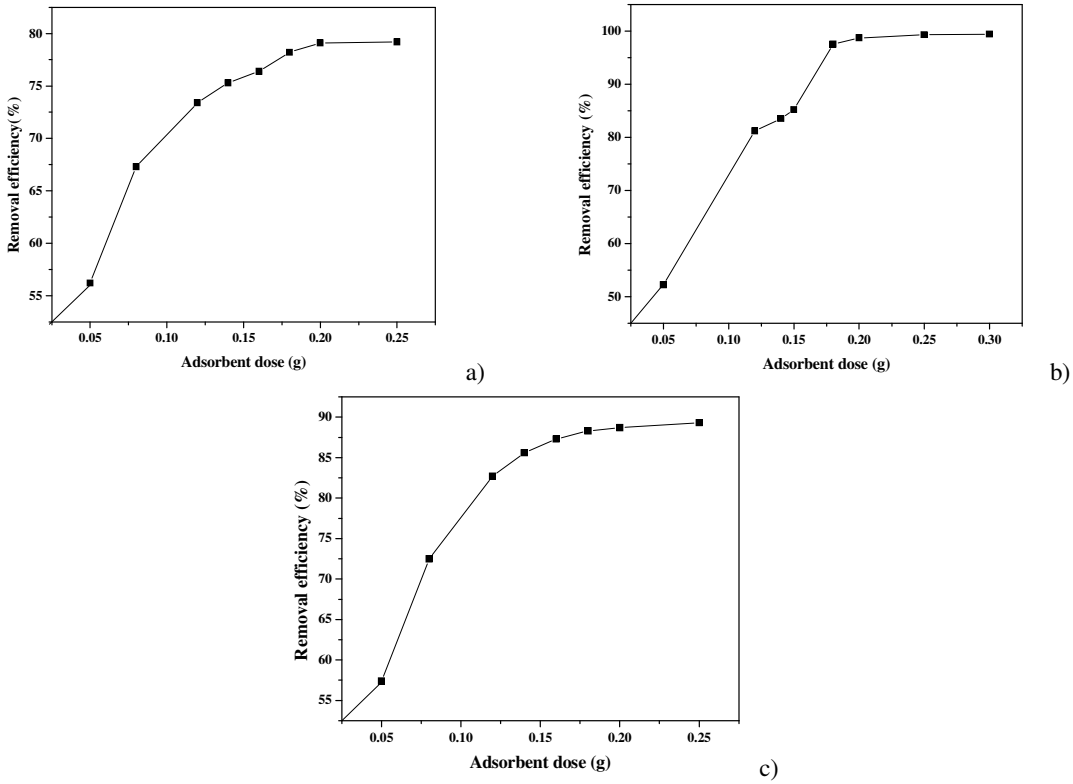

Figure 9: Effect of adsorbent dose on adsorption of a) MG, b) MB, and c) RB onto RSS

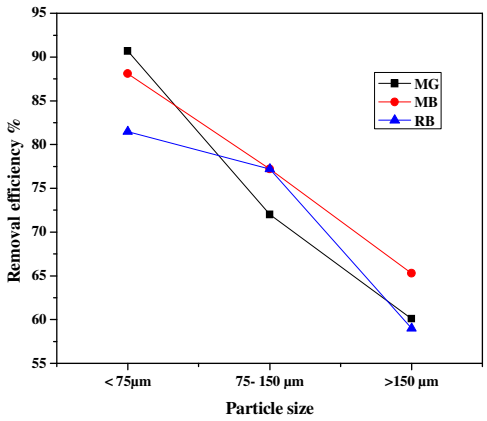

Figure 10: Effect of particle size on MG, MB and RB removal by RSS

Effect of adsorbent dose

The adsorbent dosage represents an important parameter due to its strong effect on the adsorption capacity of an adsorbent at a given initial concentration of an adsorbate.[31] The effect of the RSS adsorbent dose on the removal of the dyes studied is presented in Figure 9. It can be observed that the dye removal increases with an increment in adsorbent dosage. The increase in the percentage of dye removal with the increase in adsorbent dose might be attributed to an increase in the surface area of the adsorbent and in the number of adsorption sites available for adsorption.

Effect of particle size

The contact surface between the adsorbent and the adsorbate plays a major role in the process of adsorption. The adsorption rate of the dyes MG, MB and RB was examined for three different particle sizes of RSS (<75 µm, 75-150 µm and >150 µm), while keeping the other parameters concerning the dyes constant. The variation of the adsorption capacity (c) various particle sizes is shown in Figure 10.

The adsorption rate increased with a decrease in particle size. This is attributed to the availability of a larger surface area, which means greater accessibility of a higher number of active sites present in the adsorbent. The breaking up of large particles into smaller ones opens some tiny sealed channels, which might then become available for adsorption, leading to increased adsorption in smaller particles, compared to larger ones.[32] In the case of larger particles, the diffusion resistance to mass transport is higher and most of the internal surface of the particles may not be utilized for adsorption.[23]

Isotherm studies

Langmuir adsorption isotherm

The Langmuir adsorption isotherm has been successfully applied to many adsorption processes and assumes monolayer adsorption onto a surface containing a finite number of adsorption sites, using uniform strategies of adsorption, with no transmigration of the adsorbate in the plane of the surface.[33,34] The Langmuir isotherm is represented by the following equation:[35]

$$C_e/q_e = 1/Q_0b + C_e/Q_0 \quad (2)$$

where C_e (mg/L) is the equilibrium concentration of the dye, q_e (mg/g) is the amount of dye adsorbed at equilibrium time and Q_0 and b are Langmuir constants related to adsorption capacity and energy of adsorption, respectively. The Langmuir constants Q_0 and b can be calculated from the slope and intercept of the linear plot of C_e/q_e versus C_e. The Langmuir adsorption isotherms for the adsorption of the dyes MG, MB and RB onto RSS are shown in Figure 11 and the isotherm parameters are given in Table 3.

The Langmuir adsorption capacity, Q_0, of the dyes MG, MB and RB for the adsorption onto RSS was found to be 200, 76.92 and 33.33 mg/g, respectively. The essential characteristics of the Langmuir adsorption isotherm can be expressed in terms of a dimensionless constant separation factor or equilibrium parameter R_L defined by:

$$R_L = 1/ (1+K_LC_0) \quad (3)$$

where C_0 is initial dye concentration (mg/L) and K_L is the Langmuir constant (L/mg). R_L values indicate whether the adsorption is unfavorable (R_L = > 1), linear (R_L = 1), favorable (0 < R_L < 1), or irreversible (R_L = 0).[35] The R_L values presented in Table 3 clearly show the favorable adsorption of all three dyes onto RSS. A comparison of the

adsorption capacities (Q_0) of various adsorbents reported in the literature is presented in Table 4.

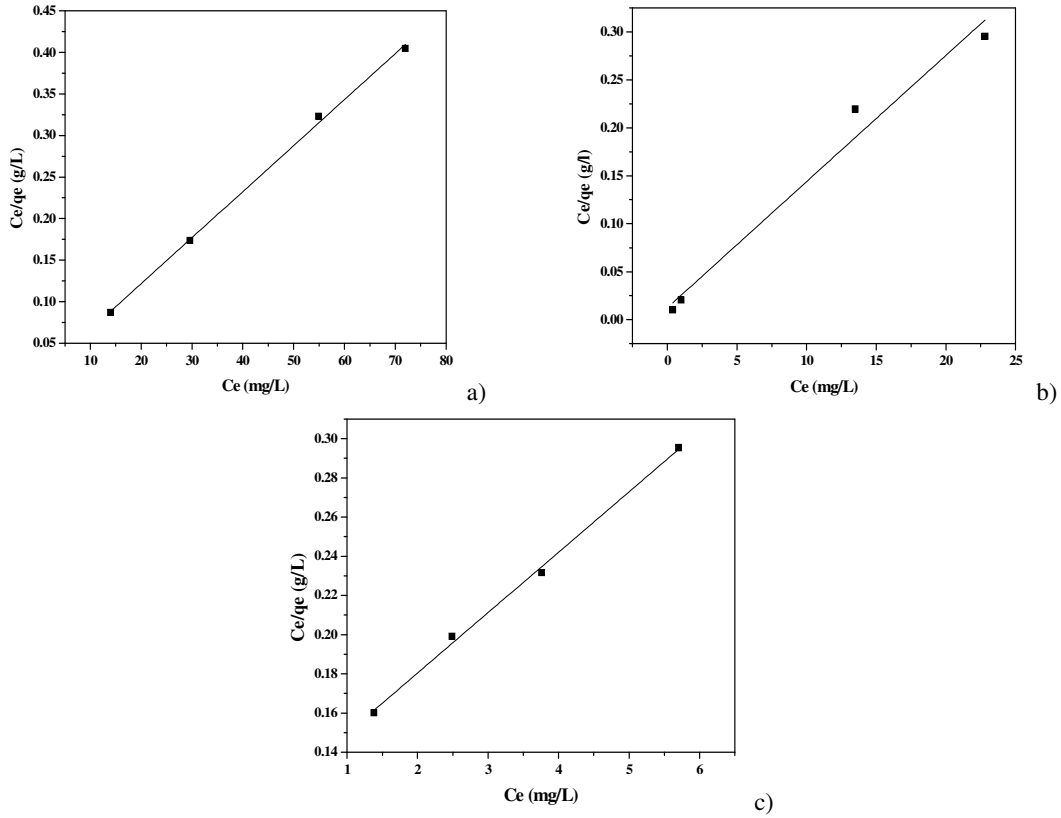

Figure 11: Langmuir adsorption isotherm for the adsorption of a) MG, b) MB, and c) RB onto RSS

Freundlich adsorption isotherm

The Freundlich isotherm model is the earliest known equation describing the adsorption process. It is an empirical equation that can be used for non-ideal sorption, which involves heterogeneous adsorption. The Freundlich isotherm can be derived assuming a logarithmic decrease in the enthalpy of adsorption with the increase in the fraction of occupied sites and is commonly given by the following non-linear equation:[32]

$$q_e = K_f C_e \, 1/n \qquad (4)$$

where K_f and n are Freundlich constants, where K_f (L/g) is the adsorption capacity of an adsorbent and shows the strength between the adsorbate and the adsorbent, while the value of n (g/L) indicates the favorability of the adsorption process.

The value of 1/n indicates the adsorption intensity of the dye onto the adsorbent and values closer to zero denote surface heterogeneity. A value of 1/n below 1 indicates favorable adsorption, while 1/n above 1 is indicative of cooperative adsorption.[33] The linear form of the equation is expressed as:

$$\ln q_e = \ln K_f + 1/n \ln C_e \qquad (5)$$

The values of K_f and n were calculated from the intercept and the slope of the linear plot of ln q_e vs ln C_e, and are given in Table 3.

The value of K_f indicates the affinity of the dyes towards the adsorbent, the greater the value of K_f, the greater is the affinity of the dyes. In the present work, MG has the highest K_f value, of 140.75 (L/g), compared to the other dyes, which shows that MG has a higher affinity to the adsorbent. The values of 1/n for all the dyes studied were below one, which indicates favorable adsorption.

Temkin isotherm

The Temkin isotherm equation contains a factor that explicitly takes into account adsorbing species–adsorbate interactions. It assumes that the heat of adsorption of all the molecules in the layer

would decrease linearly with coverage due to adsorbate–adsorbate repulsions and the adsorption is a uniform distribution of maximum binding energy.[36] The non-linear form of the Temkin isotherm is commonly represented as:[37]

$$q_e = RT/b \ln (K_t C_e) \quad (6)$$

The linear form of Temkin isotherm is expressed as:

$$q_e = B_1 \ln K_t + B_1 \ln C_e \quad (7)$$

where $B_1 = RT/b$, Kt is the equilibrium binding constant (L/mol) corresponding to the maximum binding energy and B_1 is related to the heat of adsorption. The above constants are determined using the plot of q_e vs ln C_e. The values of constants K_t and b are given in Table 3.

Table 3
Isotherm parameters for adsorption of MG, MB and RB onto RSS

Isotherm/Dye		Malachite green	Methylene blue	Rhodamine B
Langmuir	Q_0 (mg/g)	200.0	76.92	33.33
	b (L/mg^{-1})	0.500	1.083	0.250
	R^2	0.998	0.979	0.997
	R_L	0.0039	0.0046	0.074
Freundlich	K_F(L/g)	140.75	45.20	7.286
	n	19.23	6.580	1.733
	R^2	0.854	0.931	0.992
Temkin	K_T (L/g)	8.816	8.283	7.628
	b (kJ/mol)	302.1	267.7	2.185
	R^2	0.851	0.916	0.996
D-R	Q_m (mol/g)	273.14	66.02	13.37
	E (kJ/mol)	0.408	2.886	1.000
	R^2	0.810	0.846	0.948

Table 4
Comparison of maximum adsorption capacities of various low-cost adsorbents for MG, MB and RB

Adsorbent	Dye	Q_0 (mg/g)	References
RSS	MG	200.0	This study
RSS	MB	76.92	This study
RSS	RB	33.33	This study
Lotus leaf	MG	113.8	41
Wood apple shell	MG	34.56	48
Walnut shell	MG	90.8	10
Ashoka leaf powder	MG	83.3	43
Green pea peels	MB	163.94	36
Rice husk	MB	8.07	44
Silkworm exuviae	MB	25.53	25
Modified wheat straw	MB	257.8	50
Sago waste	RB	16.1	28
Turbinaria conoides	RB	80	30
Jute stick powder	RB	87.7	46
Ashoka leaf powder	RB	66.6	43

Dubinin–Radushkevich (D-R) isotherm

The D-R isotherm is more general because it does not assume a homogenous surface or constant adsorption potential and is applied to estimate the porosity, apparent free energy and the characteristics of adsorption. The linear form of the D-R isotherm is represented as:[38]

$$\ln Q_e = \ln Q_m - \beta\varepsilon^2 \quad (8)$$

where Q_m is the maximum adsorption capacity (mg g^{-1}), β is the D-R isotherm constant and ε is the Polanyi potential. The constants β (mol^2 KJ^{-2}) and Q_m (mg g^{-1}) can be calculated from the slope and intercept of the plot ln q_e vs ε^2 and are presented in Table 3. The Polanyi potential, ε, represents the work required to remove a molecule from its location and can be calculated as follows:

$$\varepsilon = RT \ln (1 + 1/C_e) \quad (9)$$

The mean free energy of adsorption (E) is the free energy when one mole of ions is transferred from infinity in solution to the surface of the sorbent. E is calculated as follows:

$$E = (-2\beta)^{1/2} \quad (10)$$

The value of E would provide information about the nature of adsorption – whether it is physisorption or chemisorption. The adsorption process is physisorption when E lies between 1 and 8 KJ mol^{-1}, while it is chemisorption when E is higher than 8 KJ mol^{-1}. The D-R isotherm parameters are presented in Table 3. From Table 3, it is clear that the values of E lie in the range from 0.408 to 2.886 KJ mol^{-1}, confirming that a weak physical force of interaction is the driving force of the adsorption of dyes onto RSS.

The isotherm parameters summarized in Table 3 reveal that the Langmuir adsorption isotherm model has a higher correlation coefficient R^2 than the other models studied. The best fit of the Langmuir isotherm clearly indicates the monolayer coverage of the dye molecules onto the outer surface of the adsorbent.

Adsorption kinetics

The rate at which adsorption takes place is of utmost importance when designing batch adsorption systems, consequently, it is important to establish the time dependence of such systems under process conditions.[39] The adsorption kinetics were analyzed using pseudo-first order, pseudo-second order, Weber-Morris intraparticle diffusion and Boyd models. The conformity between the experimental data and the model predicted values was expressed by the correlation coefficient (R^2) values. A relatively high R^2 value indicates that the model successfully describes the kinetics of adsorption.

Pseudo-first order model

The pseudo-first order model is the earliest known model suggested for the sorption of liquid/solid systems based on solid capacity. The Lagergren rate equation is the most widely used adsorption rate equation for adsorption from aqueous solutions. The Lagergren pseudo-first order model can be represented as:

$$\frac{dq_t}{dt} = k_1(q_e - q_t) \quad (11)$$

A linear form of the pseudo-first order model is represented as follows:[40]

$$\log (q_e - q_t) = \log q_e - (K_1 t)/ 2.303 \quad (12)$$

where q_e and q_t are the amount of dye adsorbed at equilibrium and at time t (mg/g), respectively, and K_1 (min^{-1}) is the rate constant of adsorption. The values of K_1 and q_e^{cal} were calculated from the slope and intercept of the plot of log ($q_e - q_t$) vs t, respectively. The values of the pseudo-first order rate constant K_1 and q_e^{cal} were determined and the correlation coefficients R^2 were presented in Table 5. A comparison of q_e^{cal} and q_e^{exp} values, and the correlation coefficients R^2 presented in Table 5 indicate the poor fit of the pseudo-first order model for all the dyes studied.

Pseudo-second order model

The adsorption may also be described by the pseudo-second order kinetic model, if the adsorption does not follow the first order kinetics.

The second order kinetic model is represented as:[41]

$$\frac{dq_t}{dt} = k_2(q_e - q_t)^2 \quad (13)$$

The linear form of the pseudo-second order model is represented as:

$$t/q_t = 1/K_2 q_e^2 + t/q_e \quad (14)$$

where K_2 is the rate constant of adsorption (g/mg min), q_e and q_t are the amount of dye adsorbed (mg/g) at equilibrium and time t (min). The values of K_2 and q_e^{cal} were calculated from the intercept ($1/K_2 q_e^2$) and slope ($1/q_e$) of the plot t/q_t vs t, respectively. The pseudo-second order plots for the adsorption of MG, MB and RB onto RSS are presented in Figure 12.

The pseudo-second order parameters, such as rate constant K_2, q_e^{cal} and correlation coefficient R^2, are presented in Table 5. It was observed that the correlation coefficient R^2 values for the pseudo-second order model were higher that the R^2 values for the pseudo-first order model. The q_e^{cal} values of all the dyes were found to be in good agreement with the q_e^{exp} values of the adsorbents. The good agreement of q_e^{cal} values with q_e^{exp} values and the high R^2 values of the pseudo-second order model confirm that the adsorption of the MG, MB and RB dyes onto RSS follows the pseudo-second order mechanism.

Table 5
Kinetic parameters for the adsorption of MG, MB and RB onto RSS at different initial concentrations

Dyes	Conc. (mg/L)	q_e^{exp} (mg/g)	Pseudo-first order			Pseudo-second order			Intraparticle diffusion	
			q_e^{cal} (mg/g)	K_1 (min^{-1})	R^2	q_e^{cal} (mg/g)	K_2 (g/mg min)	R^2	K_2 (mg/g $min^{1/2}$)	R^2
MG	350	161.0	20.13	0.066	0.960	166.6	0.009	1	2.278	0.781
	400	170.4	39.72	0.101	0.978	200.0	0.005	1	3.415	0.681
	450	170.1	36.39	0.075	0.994	200.0	0.004	0.999	3.492	0.828
	500	178.0	48.31	0.078	0.983	200.0	0.003	0.999	4.579	0.810
MB	75	37.12	9.440	0.055	0.907	37.03	0.018	0.999	1.910	0.887
	100	49.00	13.84	0.062	0.786	52.63	0.008	0.995	2.038	0.886
	150	61.50	6.970	0.053	0.971	62.50	0.019	0.999	1.341	0.963
	200	77.20	11.61	0.083	0.942	83.33	0.014	0.999	1.736	0.972
RB	20	8.260	2.198	0.034	0.995	8.849	0.047	0.999	0.183	0.830
	30	12.51	3.069	0.030	0.994	12.82	0.026	0.999	0.282	0.899
	40	16.24	3.908	0.032	0.986	16.66	0.022	0.999	0.359	0.870
	50	19.30	5.296	0.028	0.992	20.00	0.013	0.999	0.489	0.924

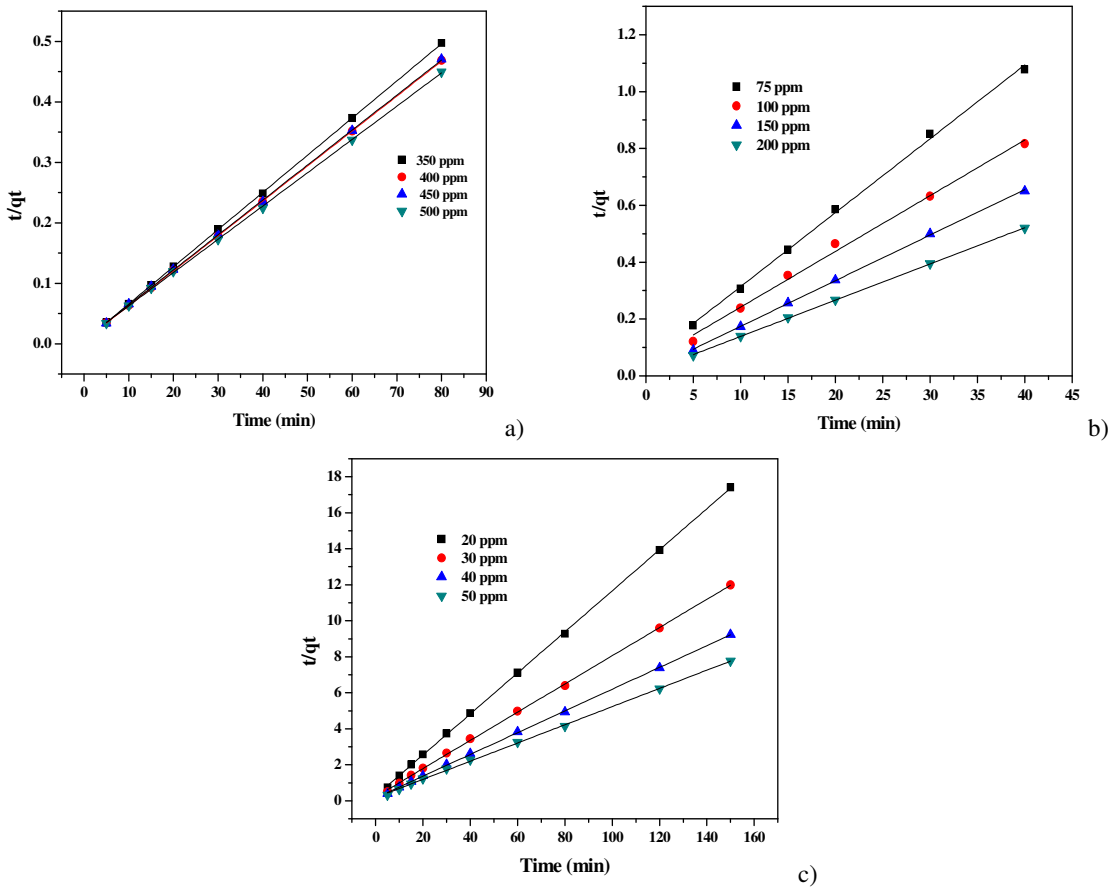

Figure 12: Pseudo-second order plots for the adsorption of a) MG, b) MB, and c) RB onto RSS

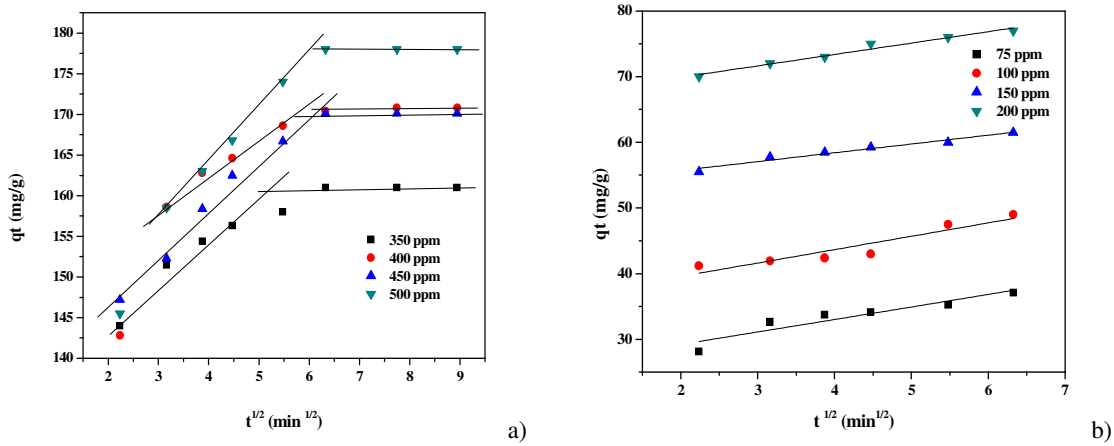

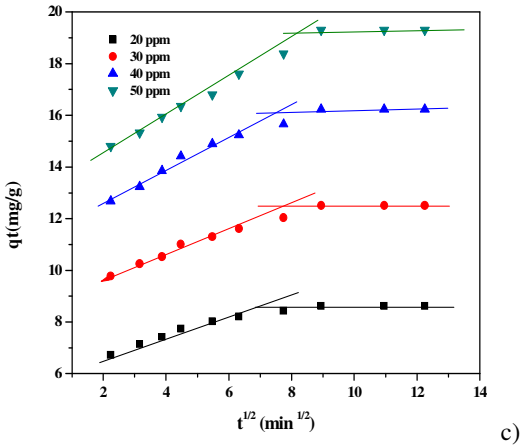

Figure 13: Intraparticle diffusion plots for the adsorption of a) MG, b) MB, and c) RB onto RSS

Intraparticle diffusion studies

In a solid liquid adsorption process, the transfer of solute from the liquid phase is usually characterized by either external mass transfer (boundary layer diffusion) or intraparticle diffusion or both. In order to investigate the diffusion mechanism and the rate controlling steps affecting the kinetics of adsorption, the kinetic data were fitted to Weber's intraparticle diffusion model.

Weber and Morris proposed an empirical relationship according to which, if intraparticle diffusion is the rate-controlling factor, the uptake of dyes varies with the square root of time.[23] The intraparticle diffusion model is expressed as:

$$q_t = K_{id}t^{1/2} + C_i \quad (15)$$

where K_{id} is the intraparticle diffusion constant ($mg/gmin^{1/2}$) and C_i is the intercept (mg/g). According to the intraparticle diffusion model equation, a plot of q_t vs $t^{1/2}$ should be a straight line with a slope K_{id} and intercept C_i, when the adsorption mechanism follows the intraparticle diffusion process. For the intraparticle diffusion model, it is essential that the plots of q_t vs $t^{1/2}$ should go through the origin, if the intraparticle diffusion is the sole rate-limiting step.[23] Boundary layer thickness is represented by C_i. Higher values of C_i correspond to a greater boundary layer.

The intraparticle diffusion plots (q_t versus $t^{1/2}$) of MG, MB and RB adsorption onto RSS are shown in Figure 13 and intrapaticle diffusion parameters are presented in Table 5. The linearity of the plots clearly indicates that intraparticle diffusion plays a significant role in the uptake of dyes MG, MB and RB by RSS. In the present study, none of the plots passed through the origin, indicating that, though intraparticle diffusion is involved in the adsorption process, it was not the sole rate-limiting step. The adsorption of MB on RSS was linear over the whole time (Fig. 13), which is attributed to macropore diffusion, involving the instantaneous utilization of the most readily available adsorbing sites on the adsorbent surface.[37] The non-zero intercept of the plots also reveals the co-existence of external film and intraparticle diffusions during the adsorption process.[42]

The linear plots of qt versus $t^{1/2}$ for the adsorption of dyes MG and RB onto RSS show that the adsorption involves a two-step process. The first step involves the adsorption of dyes on the external surface of the adsorbent (film diffusion), whereas the second step represents the diffusion of dyes to the interior of the adsorption sites (intraparticle diffusion).[23,43] Similar observations have been made regarding the adsorption of methylene blue,[44,45] malachite green, rhodamine B and brilliant green onto asoka leaf powder,[43] walnut shell,[10] bagasse pith activated carbon,[29] jute stick powder.[46]

Boyd model

The Boyd model was used to analyze the kinetic data to predict the actual slow step involved in the adsorption process. The Boyd model reveals whether the adsorption is controlled by particle diffusion, where the adsorbate transport occurs within the pores, or by film diffusion, in which the transport occurs on the external surface.[10]

Boyd equation is presented as:

$$B_t = - 0.4977 - \ln (1-F) \quad (16)$$

where F is equivalent to q_t/q_e, which represents the fraction of adsorbate adsorbed at different time, and B_t is the mathematical function of F.

According to the Boyd model, the adsorption process is controlled by particle diffusion if the linear plot of B_t vs t passes through the origin. If the linear plot does not pass through the origin, then the adsorption process is controlled by film diffusion. The plots of B_t vs t for the adsorption of dyes MG, MB and RB onto RSS are shown in Figure 14.

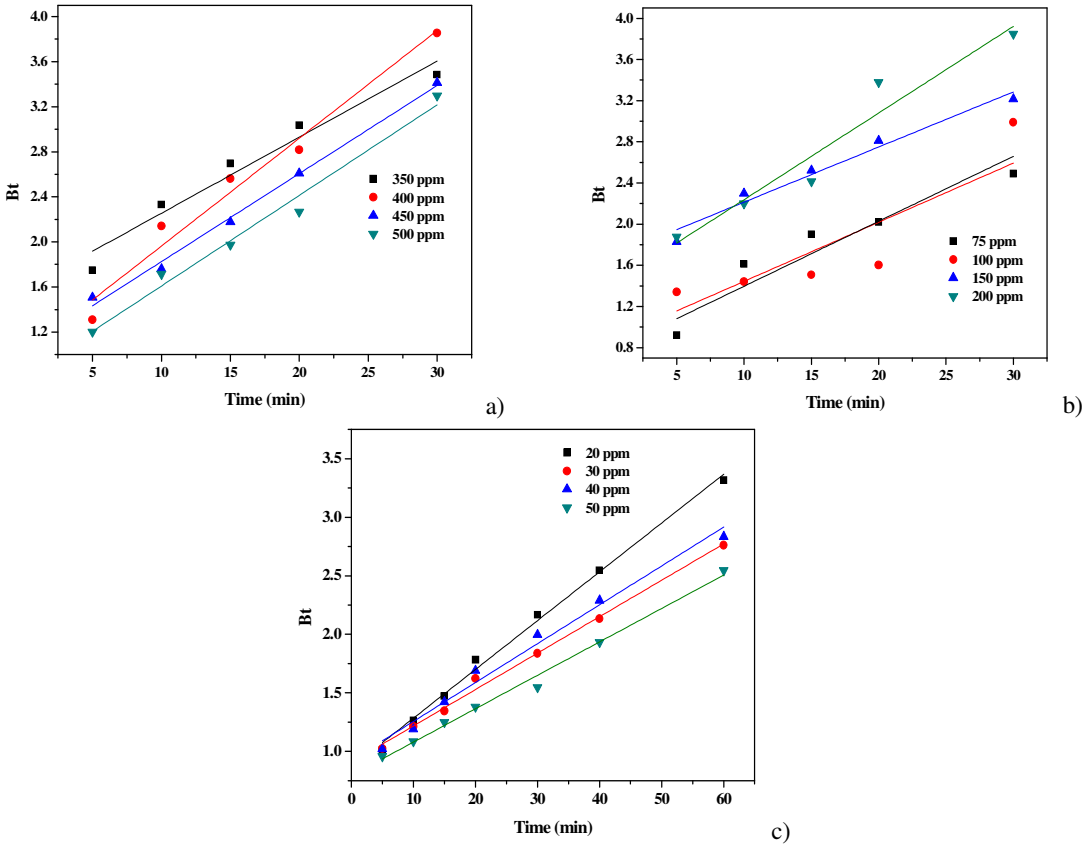

Figure 14: Boyd plots for the adsorption of a) MG, b) MB, and c) RB onto RSS

The linear plot of B_t vs t for all the dyes studied does not pass through the origin, suggesting that the adsorption process might be controlled by film diffusion. Similar results have been reported in the literature for the adsorption of malachite green on walnut shell,[10] rattan saw dust[47] and wood apple shell.[48]

Desorption studies

The regeneration of the adsorbents is a very significant step in making the adsorption process more economical for industrial applications. The mechanism of adsorption and possible recovery of the adsorbate and of the adsorbent were investigated by conducting desorption studies. Distilled water, hydrochloric acid (0.1M) and acetic acid (0.1M) were used for the desorption of the dyes MG, MB and RB. The desorption studies were carried out at 30 ± 2 °C. Table 6 shows the desorption efficiency of RSS with respect to the three dyes: MG, MB and RB. If the dye adsorbed can be desorbed by water, a weak interaction exists between the dye molecules and the adsorbent. If strong acids, such as HCl, can desorb the dye, the interaction would be of the ion exchange type. The adsorption process might be chemisorption if the dye adsorbed can be desorbed by a weak acid, such as CH_3COOH.[25,29,49] In the case of MG, higher desorption takes place in CH_3COOH, suggesting

the chemisorption of MG. The dyes MB and RB show higher desorption in HCl, compared to distilled water and CH_3COOH, suggesting the ion exchange mechanism of adsorption of both dyes. Similar behavior has been observed for MB in silkworm exuviae,[25] wheat straw materials,[50] citric acid modified kenaf fibres.[42]

Studies related to the removal of dyes from synthetic wastewater

The wastewater from textile manufacturing or dye processing industries usually contains various types of suspended and dissolved compounds, apart from dyes. Metal cations, such as Na^+, K^+, Cu^{2+}, and Ca^{2+}, are the most common metal ions present in wastewater. The presence of these metal ions leads to high ionic strength, which may significantly affect the efficiency of the adsorption process.[51] To investigate the potential of the adsorbent for industrial wastewater, synthetic wastewater containing all the three dyes studied was prepared and its composition is presented in Table 7. The percent removal of the synthetic dye mixture increased with the increase in adsorbent dosage and the maximum color removal was observed at an adsorbent dose of 14 g/L.

Table 6
Desorption efficiency of the adsorbents

Dyes	MG	MB	RB
Dye concentration (mg/L)	500	200	50
Adsorbent dose (g)	0.2	0.2	0.2
Equilibrium time (min)	60	60	80
Removal efficiency (%)	92	98.7	87.6
Desorption efficiency in H_2O (%)	16.5	0.526	3.1
Desorption efficiency in HCl (%)	20	31.15	27.4
Desorption efficiency in CH_3COOH (%)	40	26.23	10.3

Table 7
Composition of synthetic wastewater containing the three dyes

Characteristics	Values
pH	11.0
Conductivity (mS/cm)	0.109
Sodium (mg/L)	1110
Calcium (mg/L)	700
Potassium (mg/L)	950
Iron (mg/L)	20
Malachite green (mg/L)	50
Methylene blue (mg/L)	50
Rhodamine B (mg/L)	10

Figure 15 shows the effect of pH on the color removal of synthetically prepared dye wastewater and the single dye solutions. The percent color removal decreased with the increase in pH from 2 to 11. This might be attributed to the fact that wastewater is associated with presence of various ions, such Na^+, Ca^{2+}, K^+ and Fe^{2+}, which could compete with positively charged dye molecules for the same binding sites on the adsorbent surface in the wastewater.[52]

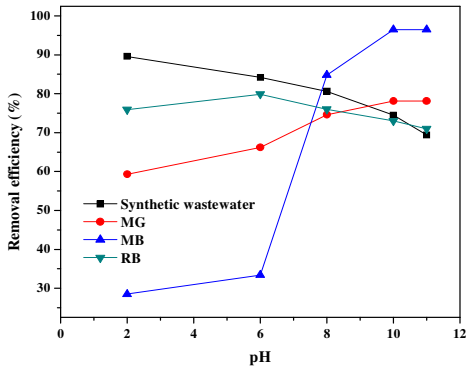

Figure 15: Effect of pH on the adsorption of synthetic wastewater and dyes MG, MB and RB by RSS

CONCLUSION

Simarouba glauca seed shell powder can be used as an efficient adsorbent for the removal of dyes Malachite green, Methylene blue and Rhodamine B from aqueous solutions. The isotherm data fitted well the Langmuir isotherm, with maximum adsorption capacity values of 200, 76.92 and 33.33 mg/g for MG, MB and RB, respectively. The adsorption of the dyes followed second-order rate expression and the process of adsorption might be due to film diffusion. Desorption studies revealed the mechanism of dye adsorption. Malachite green followed the chemisorption mechanism, whereas Methylene blue and Rhodamine B followed the ion exchange mechanism.

REFERENCES

[1] V. Gupta and Suhas, *J. Environ. Manage*., **90**, 2313 (2009), https://doi.org/10.1016/j.jenvman.2008.11.017

[2] V. I. Grover, "Water Global Common and Global Problems", Enfield, NH, Science Publishers, 2006, https://thesciencepublishers.com

[3] W. Zhang, H. Li, X. Kan, L. Dong, H. Yan *et al*., *Bioresour. Technol*., **117**, 40 (2012), https://doi.org/10.1016/j.biortech.2012.04.064

[4] J. Song, W. Zou, Y. Bian, F. Su and R. Han, *Desalination*, **265**, 119 (2011), https://doi.org/10.1016/j.desal.2010.07.041

[5] V. Garg, R. Kumar and R. Gupta, *Dyes Pigments*, **62**, 1 (2004), https://doi.org/10.1016/j.dyepig.2003.10.016

[6] G. Mckay, *J. Chem. Technol. Biotechnol*., **32**, 759 (1982), https://doi.org/10.1002/jctb.5030320712

[7] S. M. D. O. Brito, H. M. C. Andrade, L. F. Soares and R. P. D. Azevedo, *J. Hazard. Mater*., **174**, 84 (2010), https://doi.org/10.1016/j.jhazmat.2009.09.020

[8] S. Jain and R. V. Jayaram, *Desalination*, **250**, 921 (2010), https://doi.org/10.1016/j.desal.2009.04.005

[9] J. Shah, M. R. Jan, A. Haq and Y. Khan, *Front. Chem. Sci. Eng*., **7**, 428 (2013), https://doi.org/10.1007/s11705-013-1358-x

[10] M. K. Dahri, M. R. R. Kooh and L. B. Lim, *J. Environ. Chem. Eng*., **2**, 1434 (2014), https://doi.org/10.1016/j.jece.2014.07.008

[11] C. K. Enenebeaku, N. J. Okorocha and A. O. Chris, *Am. J. Chem. Mater. Sci*., **2**, 14 (2015), http://www.openscienceonline.com/journal/ajcms

[12] S. Saroj, S. V. Singh and D. Mohan, *Arab. J. Sci. Eng*., **40**, 1553 (2015), https://doi.org/10.1007/s13369-015-1630-0

[13] M. R. Malekbala, S. Hosseini, S. K. Yazdi, S. M. Soltani and M. R. Malekbala, *Chem. Eng. Res. Des*., **90**, 704 (2012), https://doi.org/10.1016/j.cherd.2011.09.010

[14] C. Namasivayam and D. Kavitha, *Dyes Pigm*., **54**, 47 (2002), https://doi.org/10.1016/S0143-7208(02)00025-6

[15] V. Garg, *Dyes Pigm*., **63**, 243 (2004), https://doi.org/10.1016/j.dyepig.2004.03.005

[16] H. Wang, X. Yuan, Z. Wu, L. Wang, X. Peng *et al*., *Sep. Purif. Technol*., **49**, 2689 (2014), https://doi.org/10.1080/01496395.2014.940590

[17] K. A. G. C. A. Gusmão, L. V. A. Gurgel, T. M. S. Melo and L. F. Gil, *Dyes Pigm*., **92**, 967 (2012), https://doi.org/10.1016/j.dyepig.2011.09.005

[18] P. Devan and N. Mahalakshmi, *Fuel*, **88**, 1828 (2009), https://doi.org/10.1016/j.fuel.2009.04.025

[19] C.-H. Weng, Y.-T. Lin and T.-W. Tzeng, *J. Hazard. Mater*., **170**, 417 (2009), https://doi.org/10.1016/j.jhazmat.2009.04.080

[20] K. A. Krishnan and A. Haridas, *J. Hazard. Mater*., **152**, 527 (2008), https://doi.org/10.1016/j.jhazmat.2007.07.015

[21] E. K. Radwan, M. B. M. Ibrahim, A. S. Moursy and H. H. Abdel Ghafar, *J. Environ. Sci. Technol*., **12**, 221 (2019), https://doi.org/10.3923/jest.2019.221.227

[22] Y. Feng, H. Zhou, G. Liu, J. Qiao, J. Wang *et al*., *Bioresour. Technol*., **125**, 138 (2012), https://doi.org/10.1016/j.biortech.2012.08.128

[23] M. Doğan, H. Abak and M. Alkan, *J. Hazard. Mater*., **164**, 172 (2009), https://doi.org/10.1016/j.jhazmat.2008.07.155

[24] M. A. Ahmad and R. Alrozi, *Chem. Eng. J*., **171**, 510 (2011), https://doi.org/10.1016/j.cej.2011.04.018

[25] H. Chen, J. Zhao and G. Dai, *J. Hazard. Mater.*, **186**, 1320 (2011), https://doi.org/10.1016/j.jhazmat.2010.12.006
[26] M. Fernandez, G. Nunell, P. Bonelli and A. Cukierman, *Bioresour. Technol.*, **101**, 9500 (2010), https://doi.org/10.1016/j.biortech.2010.07.102
[27] C. Namasivayam, M. D. Kumar, K. Selvi, R. A. Begum, T. Vanathi *et al.*, *Biomass Bioenerg.*, **21**, 477 (2001), https://doi.org/10.1016/S0961-9534(01)00052-6
[28] K. Kadirvelu, C. Karthika, N. Vennilamani and S. Pattabhi, *Chemosphere*, **60**, 1009 (2005), https://doi.org/10.1016/j.chemosphere.2005.01.047
[29] H. M. Gad and A. A. El-Sayed, *J. Hazard. Mater.*, **168**, 1070 (2009), https://doi.org/10.1016/j.jhazmat.2009.02.155
[30] S.-L. Hii, S.-Y. Yong and C.-L. Wong, *J. Appl. Phycol.*, **21**, 625 (2009), https://doi.org/10.1007/s10811-009-9448-3
[31] T. K. Sen, S. Afroze and H. M. Ang, *Water Air Soil Pollut.*, **218**, 499 (2010), https://doi.org/10.1007/s11270-010-0663-y
[32] E.-K. Guechi and O. Hamdaoui, *Desalin. Water. Treat.*, **51**, 3371 (2013), https://doi.org/10.1080/19443994.2012.749191
[33] T. Santhi, S. Manonmani and T. Smitha, *J. Hazard. Mater.*, **179**, 178 (2010), https://doi.org/10.1016/j.jhazmat.2010.02.076
[34] L. Wang, J. Zhang, R. Zhao, C. Li, Y. Li *et al.*, *Desalination*, **254**, 68 (2010), https://doi.org/10.1016/j.desal.2009.12.012
[35] C. Namasivayam and R. Yamuna, *Water Air Soil Pollut.*, **113**, 371 (1999), https://doi.org/10.1023/A:1005080301379
[36] R. Dod, G. Banerjee and S. Saini, *Biotechnol. Bioprocess. Eng.*, **17**, 862 (2012), https://doi.org/10.1007/s12257-011-0614-5
[37] D. Kavitha and C. Namasivayam, *Bioresour. Technol.*, **98**, 14 (2007), https://doi.org/10.1016/j.biortech.2005.12.008
[38] H. E. Bakouri, J. Usero, J. Morillo and A. Ouassini, *Bioresour. Technol.*, **100**, 4147 (2009), https://doi.org/10.1016/j.biortech.2009.04.003
[39] Y.-S. Ho, *Water Res.*, **40**, 119 (2006), https://doi.org/10.1016/j.watres.2005.10.040
[40] C. Xia, Y. Jing, Y. Jia, D. Yue, J. Ma *et al.*, *Desalination*, **265**, 81 (2011), https://doi.org/10.1016/j.desal.2010.07.035
[41] X. Han, J. Yuan and X. Ma, *Desalin. Water. Treat.*, **52**, 5563 (2014), https://doi.org/10.1080/19443994.2013.813102
[42] M. S. Sajab, C. H. Chia, S. Zakaria, S. M. Jani, M. K. Ayob *et al.*, *Bioresour. Technol.*, **102**, 7237 (2011), https://doi.org/10.1016/j.biortech.2011.05.011
[43] N. Gupta, A. K. Kushwaha and M. Chattopadhyaya, *J. Taiwan Inst. Chem. Eng.*, **43**, 604 (2012), https://doi.org/10.1016/j.jtice.2012.01.008
[44] M.-C. Shih, *Desalin. Water. Treat.*, **37**, 200 (2012), https://doi.org/10.1080/19443994.2012.661273
[45] V. Ponnusami, S. Vikram and S. Srivastava, *J. Hazard. Mater.*, **152**, 276 (2008), https://doi.org/10.1016/j.jhazmat.2007.06.107
[46] G. C. Panda, S. K. Das and A. K. Guha, *J. Hazard. Mater.*, **164**, 374 (2009), https://doi.org/10.1016/j.jhazmat.2008.08.015
[47] B. Hameed and M. El-Khaiary, *J. Hazard. Mater.*, **159**, 574 (2008), https://doi.org/10.1016/j.jhazmat.2008.02.054
[48] A. S. Sartape, A. M. Mandhare, V. V. Jadhav, P. D. Raut, M. A. Anuse *et al.*, *Arab. J. Chem.*, **10**, S3329 (2017), https://doi.org/10.1016/j.arabjc.2013.12.019
[49] C. Namasivayam, N. Muniasamy, K. Gayatri, M. Rani and K. Ranganathan, *Bioresour. Technol.*, **57**, 37 (1996), https://doi.org/10.1016/0960-8524(96)00044-2
[50] W. Zhang, H. Yan, H. Li, Z. Jiang, L. Dong *et al.*, *Chem. Eng. J.*, **168**, 1120 (2011), https://doi.org/10.1016/j.cej.2011.01.094
[51] J.-X. Yu, B.-H. Li, X.-M. Sun, J. Yuan and R. Chi, *J. Hazard. Mater.*, **168**, 1147 (2009), https://doi.org/10.1016/j.jhazmat.2009.02.144
[52] A. Witek-Krowiak, *Chem. Eng. J.*, **171**, 976 (2011), https://doi.org/10.1016/j.cej.2011.04.048